BIOCHEMISTRY

Evolutionary adaptation of visual pigments in geckos for their photic environment

Keiichi Kojima[1,2], Yuki Matsutani[1], Masataka Yanagawa[3], Yasushi Imamoto[1], Yumiko Yamano[4], Akimori Wada[4], Yoshinori Shichida[1,5], Takahiro Yamashita[1]*

Vertebrates generally have a single type of rod for scotopic vision and multiple types of cones for photopic vision. Noteworthily, nocturnal geckos transmuted ancestral photoreceptor cells into rods containing not rhodopsin but cone pigments, and, subsequently, diurnal geckos retransmuted these rods into cones containing cone pigments. High sensitivity of scotopic vision is underlain by the rod's low background noise, which originated from a much lower spontaneous activation rate of rhodopsin than of cone pigments. Here, we revealed that nocturnal gecko cone pigments decreased their spontaneous activation rates to mimic rhodopsin, whereas diurnal gecko cone pigments recovered high rates similar to those of typical cone pigments. We also identified amino acid residues responsible for the alterations of the spontaneous activation rates. Therefore, we concluded that the switch between diurnality and nocturnality in geckos required not only morphological transmutation of photoreceptors but also adjustment of the spontaneous activation rates of visual pigments.

INTRODUCTION

Vertebrate eyes have two types of photoreceptor cells, rods and cones for scotopic and photopic vision, respectively (*1*, *2*). Rods and cones contain different types of visual pigments, rhodopsin and cone pigments, respectively. In the photoreceptor cells, visual pigments absorb a photon via cis-trans photoisomerization of the retinal chromophore and then activate heterotrimeric G protein (Gt) to drive the light-dependent responses of the photoreceptor cells. Scotopic vision requires extremely high sensitivity and low threshold for the ability to detect only a few photons (*3*–*5*). The light-dependent responses in rods are invariably transmitted to higher-order retinal neurons in the background of light-independent noise, which is composed of two components, discrete and continuous noise (*6*). The discrete noise originates from the thermal activation of the visual pigments, which is due to the thermal isomerization of the retinal chromophore (*6*, *7*). The continuous noise originates from the spontaneous activation of phosphodiesterase 6 (PDE6) in the phototransduction cascade (*8*, *9*). The noise level is proportional to the square root of the spontaneous activation rates. Since a rod's true single-photon response can be separated from the continuous noise but not from the discrete noise in the higher-order retinal neurons (*5*, *10*–*12*), the discrete noise level in principle constitutes an ultimate limit to visual sensitivity. Therefore, a low thermal activation rate of rhodopsin is essential for scotopic vision (*5*, *10*–*12*). Compared to rods, cones show a substantially higher noise level, which sets the absolute visual threshold in cone vision (*13*). The high noise level of cones arises predominantly from the high level of cone pigment–related noise or the overwhelming level of continuous noise by PDE6 (*9*, *14*, *15*). Thermal activations of cone pigment, whose rates are much higher than those of rhodopsin, are not visible as discrete events due to the lower gain of the phototransduction cascade in cones.

Most vertebrates have a single type of rod and multiple types of cones in their retina (Fig. 1), which allows them to see objects monochromatically at night and multichromatically during the day (*1*, *2*). Noteworthily, geckos have transmuted the morphology of their photoreceptor cells according to their activity rhythm, as recognized in the "transmutation hypothesis" of Walls (*16*). While the ancestral diurnal lizards had only cones for photopic vision, nocturnal geckos transmuted the ancestral cones into rods for scotopic vision, and then diurnal geckos retransmuted the ancestral rods into cones for photopic vision (Fig. 1). The transmutation hypothesis is supported by the observation of the morphological features of the photoreceptor cells (*17*, *18*) and the characterization of the signaling molecules expressed in the cells (*19*–*21*). In general, diurnal lizards have one rhodopsin and four types of cone pigments, that is, red-, green-, blue-, and ultraviolet (UV)–sensitive cone pigments, which are phylogenetically categorized as the L [long and middle wavelength sensitive (LWS/MWS)], M2 [rhodopsin-like (Rh2)], M1 [short wavelength sensitive 2 (SWS2)], and S [short wavelength sensitive 1 (SWS1)] groups, respectively (*22*, *23*). However, the genomic analysis of nocturnal geckos (*Gekko japonicus* and *Paroedura picta*) revealed that they have only three types of visual pigments—red-, green- and UV-sensitive cone pigments—because rhodopsin and blue-sensitive cone pigments were lost (*24*, *25*). This indicates that, in contrast to the normal rods containing rhodopsin, nocturnal

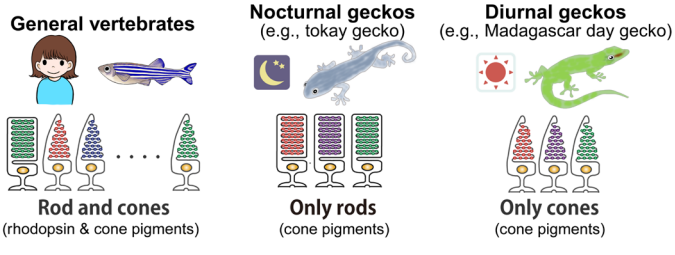

Fig. 1. Morphology of photoreceptor cells in nocturnal and diurnal geckos. Nocturnal and diurnal geckos have only rods and only cones expressing cone pigments, while vertebrates generally have a rod expressing rhodopsin and several types of cones expressing cone pigments.

[1]Department of Biophysics, Graduate School of Science, Kyoto University, Kyoto 606-8502, Japan. [2]Graduate School of Medicine, Dentistry and Pharmaceutical Sciences, Okayama University, Okayama 700-8530, Japan. [3]Cellular Informatics Laboratory, RIKEN Cluster for Pioneering Research, 2-1 Hirosawa, Wako 351-0198, Japan. [4]Laboratory of Organic Chemistry for Life Science, Kobe Pharmaceutical University, Kobe 658-8558, Japan. [5]Research Organization for Science and Technology, Ritsumeikan University, Kusatsu, Shiga 525-8577, Japan.
*Corresponding author. Email: yamashita.takahiro.4z@kyoto-u.ac.jp

gecko rods contain red-, green-, and UV-sensitive cone pigments (*19*, *24*, *26*, *27*). Besides, diurnal gecko cones contain the cognate three types of cone pigments (*27*, *28*). These molecular bases of the gecko visual system raise the open question of whether the nocturnal and diurnal geckos adapted to the light environment by the alteration of the molecular properties of cone pigments according to the transmutation of the morphology of the photoreceptor cells. In this study, we quantitatively compared the thermal activation rates of green- and UV-sensitive cone pigments among a diurnal lizard, a nocturnal gecko and a diurnal gecko. Our biochemical analysis revealed that nocturnal gecko cone pigments acquired low thermal activation rates similar to rhodopsin, and then diurnal gecko cone pigments reacquired high rates similar to typical cone pigments through several amino acid mutations. On the basis of these results, we discuss the mechanism of alteration of the molecular properties of cone pigments and their physiological implications for gecko vision.

RESULTS AND DISCUSSION

Comparison of thermal activation rates of gecko cone pigments

We previously optimized biochemical methods for estimating the thermal activation rates (k_{th}) of visual pigments using recombinant proteins expressed in mammalian cultured cells (*29*–*31*). Briefly, we can calculate the thermal activation rates of visual pigments using the following equation, which contains three experimentally determined values (fig. S1)

$$k_{th} = \frac{v_{dark}}{v_{light}} k_d \quad (1)$$

v_{dark} is the initial rate of G protein activation by a pigment in the dark, v_{light} is the initial rate of G protein activation by a photoactivated pigment, and k_d is the spontaneous decay rate of the activated pigment. The method allows us to quantitatively compare the thermal activation rates of various pigments, including mutants, in the same experimental condition. As described above, nocturnal gecko rods express red-, green-, and UV-sensitive cone pigments (*19*, *24*, *26*). To investigate whether nocturnal gecko cone pigments have altered their properties into rhodopsin-like ones, we measured the thermal activation rates of green-sensitive cone pigments from a nocturnal gecko, the tokay gecko (*Gekko gecko*), and a diurnal lizard, the green anole *(Anolis carolinensis*) (tokay gecko green and green anole green, respectively) and UV-sensitive cone pigments from them (tokay gecko UV and green anole UV, respectively) (Fig. 2 and figs. S2 to S4) since we can obtain substantial amounts of their functional pigments in mammalian cultured cells. Our results showed that the thermal activation rates of green anole green and green anole UV are 150- and 58-fold higher than that of bovine rhodopsin and are comparable to those of typical cone pigments, chicken green-sensitive cone pigment (chicken green), and tiger salamander UV-sensitive cone pigment (tiger salamander UV), respectively. In contrast, tokay gecko green and UV exhibited rhodopsin-like low thermal activation rates. Therefore, we concluded that the thermal activation rates of tokay gecko green and UV were decreased to levels typical of rhodopsin according to the transmutation from cones into rods. These low thermal activation rates of cone pigments can lead to a decrease of the discrete noise level in tokay gecko rods for scotopic vision.

Next, to investigate whether diurnal gecko cone pigments rechanged their properties into typical cone pigment–like ones, we measured the thermal activation rates of green- and UV-sensitive cone pigments of a diurnal gecko, the Madagascar day gecko (*Phelsuma madagascariensis longintinue*) (Madagascar day gecko green and UV, respectively) (Fig. 2 and figs. S2 to S4). The thermal activation rates of Madagascar day gecko green and UV were 150- and 52-fold higher than that of bovine rhodopsin and were comparable to those of chicken green and tiger salamander UV, respectively. Thus, we concluded that Madagascar day gecko green and UV increased their thermal activation rates compared with those of tokay gecko cone pigments as part of the transmutation of rods back to cones. The high thermal activation rates could achieve the increase of pigment-related noise level in Madagascar day gecko cones, which leads to a high level of cone noise for photopic vision.

In addition to geckos, it is well known that many snake species transmuted the morphology of photoreceptor cells according to their activity rhythm (*16*, *32*). A diurnal garter snake, the western ribbon snake (*Thamnophis proximus*), has only cones expressing red- and UV-sensitive cone pigments and rhodopsin (western ribbon snake red, UV, and rhodopsin, respectively) (fig. S5A) (*32*, *33*). We also investigated whether western ribbon snake visual pigments expressed in cones exhibit high thermal activation rates similar to typical cone pigments (fig. S5, B and C). Western ribbon snake UV exhibited a 69-fold higher thermal activation rate than bovine rhodopsin, similar to tiger salamander UV, whereas western ribbon snake rhodopsin exhibited a low thermal activation rate (fig. S5C). Thus, we concluded that diurnal western ribbon snake did not increase the thermal activation rate of rhodopsin expressed in cones.

Key residues for changing thermal activation rates of gecko cone pigments

To understand the molecular mechanism underlying the change of the thermal activation rates of tokay gecko cone pigments, we sought to identify key residues responsible for the low thermal activation rates of tokay gecko green and UV. We previously found that two residues, Glu^{122} and Ile^{189} (according to the bovine rhodopsin numbering system), are responsible for the low thermal activation rate of rhodopsin compared with typical cone pigments (*29*). We also found that Anura blue-sensitive cone pigments expressed in green rods exhibit the low thermal activation rate because of the acquisition of Thr^{47} not Glu^{122} and Ile^{189} (*30*). However, the amino acid sequences of tokay gecko green and UV do not conserve these amino acid residues at positions 47, 122, or 189 (fig. S6). Thus, we speculated that other amino acid residue(s) are responsible for the low thermal activation rates of tokay gecko green and UV. We first compared amino acid residues located within 8 Å of the retinal chromophore in the crystal structure of bovine rhodopsin between nocturnal gecko and other vertebrate green-sensitive cone pigments and found that four residues (at positions 213, 216, 273, and 289) were conserved only among nocturnal gecko pigments (Fig. 3A and fig. S7). Our previous studies indicated that there is a strong correlation between the thermal activation rates and the decay rates of the active state (k_d) in visual pigments (*29*, *30*). Therefore, we measured k_d of wild type and mutants of tokay gecko green to screen candidate residue(s) (fig. S9A). Among the four mutants—T213V, M216V, I273F, and T289S—of tokay gecko green, the T213V mutant had significantly increased k_d. The measurement of the thermal activation rate confirmed that the T213V mutant had a 6.2-fold increase of the rate (Fig. 3, C and E). We also compared amino acid residues located within 12 Å of the retinal chromophore in the crystal structure of

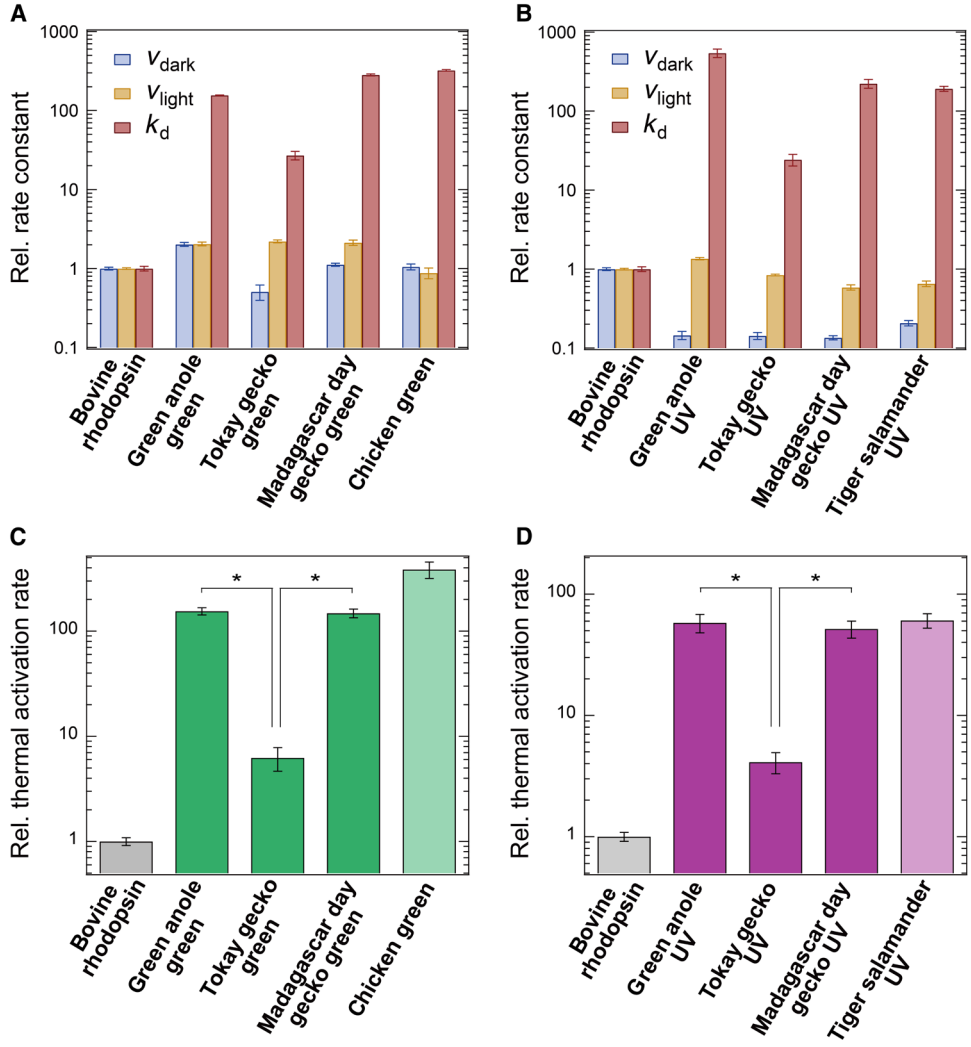

Fig. 2. Comparison of the thermal activation rates (k_{th}) of wild-type gecko visual pigments. (**A**) Comparison of v_{dark}, v_{light}, and k_d of bovine rhodopsin, green anole green, tokay gecko green, Madagascar day gecko green, and chicken green measured by the biochemical and fluorescence assays (figs. S2 to S4). (**B**) Comparison of v_{dark}, v_{light}, and k_d of bovine rhodopsin, green anole UV, tokay gecko UV, Madagascar day gecko UV, and tiger salamander UV measured by the biochemical and fluorescence assays (figs. S2 to S4). (**C**) Comparison of the thermal activation rates (k_{th}) of bovine rhodopsin, green anole, tokay gecko, Madagascar day gecko, and chicken green estimated from the data presented in (A). (**D**) Comparison of the thermal activation rates (k_{th}) of bovine rhodopsin, green anole, tokay gecko, Madagascar day gecko, and tiger salamander UV estimated from the data presented in (B). All error bars represent the SEM of more than three independent measurements. * indicates a significant difference in relative rate constants between visual pigments [Bonferroni, $P < 0.05/5$; analysis of variance (ANOVA)].

bovine rhodopsin between nocturnal gecko and other vertebrate UV/violet-sensitive cone pigments and found that three residues, at positions 89, 172, and 287, were conserved only among nocturnal gecko pigments (Fig. 3B and fig. S8). The measurement of k_d of the mutants at these positions of tokay gecko UV showed that the V89F and Y172F mutants had significantly increased k_d (fig. S9B). As expected, the V89F and Y172F mutations in tokay gecko UV increased the thermal activation rates (by 3.1- and 2.2-fold, respectively) (Fig. 3, D and F). These results suggest that Thr^{213} in tokay gecko green and Val^{89} and Tyr^{172} in tokay gecko UV are major contributors to the acquisition of these proteins' low rhodopsin-like thermal activation rates.

Second, we sought to identify key residues responsible for the high thermal activation rates of Madagascar day gecko green and UV. We compared amino acid residues located within 8 Å of the retinal chromophore in the crystal structure of bovine rhodopsin between diurnal and nocturnal gecko green-sensitive cone pigments and found that five residues, at positions 112, 168, 213, 270, and 273, were different between diurnal and nocturnal gecko pigments (Fig. 3A and fig. S7). Among the mutants at these positions (F112I, G168A, L213T, T270A, and C273I) of Madagascar day gecko green, the F112I mutant had significantly decreased k_d (fig. S9C). Moreover, the F112I mutant of Madagascar day gecko green had a 2.1-fold decreased thermal activation rate (Fig. 3, C and G). We also compared amino acid residues located within 12 Å of the retinal chromophore in the crystal structure of bovine rhodopsin between diurnal and nocturnal gecko UV-sensitive cone pigments and found that 11 residues, at positions 89, 90,169,172, 178, 184, 210, 213, 217, 263, and 298, were different between diurnal and nocturnal gecko pigments (Fig. 3B and fig. S8). We measured k_d of F89V, S90A, V169I, F172Y, Y178F, G184Q, F210L, M213I, T217S, T263L, and A298S of Madagascar day

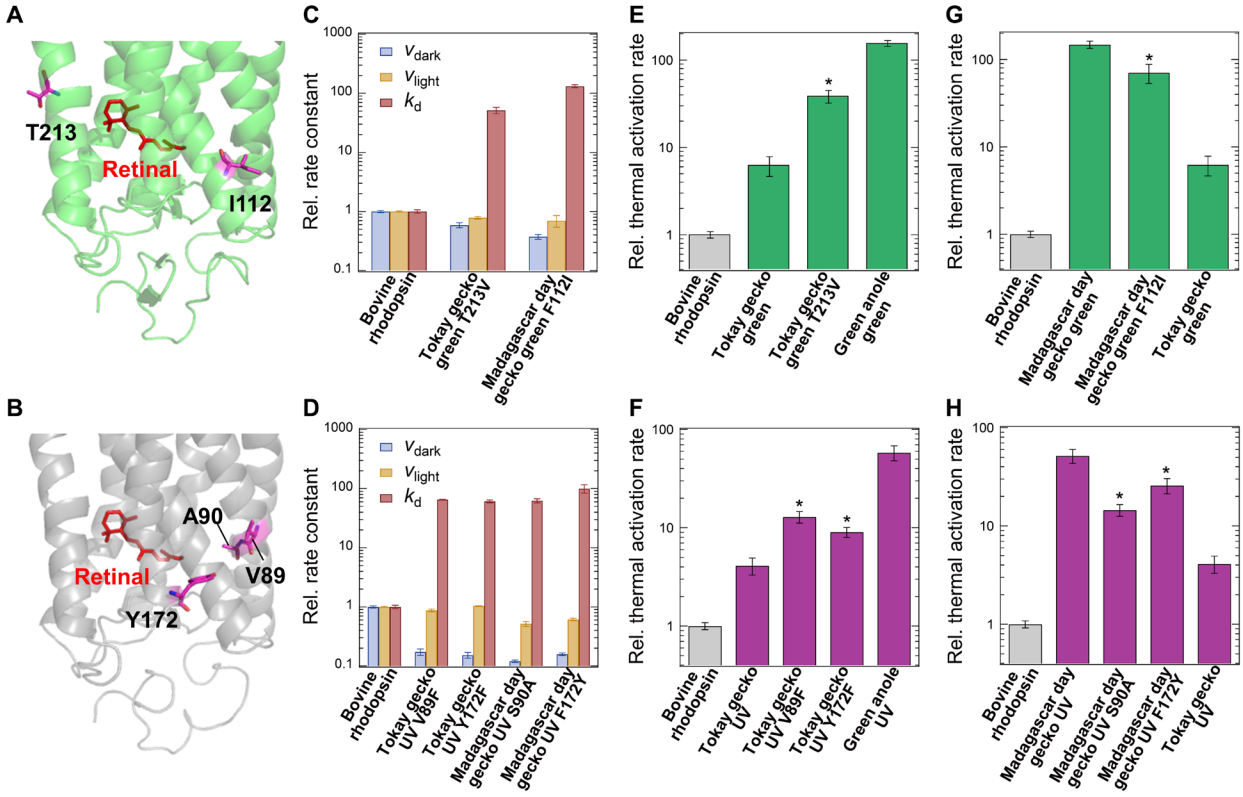

Fig. 3. Key amino acid residues regulate the thermal activation rates (k_{th}) of gecko green– and UV-sensitive cone pigments. (**A** and **B**) Homology model structures of tokay gecko green (A) and tokay gecko UV (B) that were constructed on the basis of the crystal structure of the dark state of bovine rhodopsin (Protein Data Bank: 1U19). The mutated residues (Val[89], Ala[90], Ile[112], Tyr[172], and Thr[213]) and 11-cis-retinal are colored magenta and red, respectively. (**C**) Comparison of v_{dark}, v_{light}, and k_d of bovine rhodopsin, T213V mutant of tokay gecko green, and F112I mutant of Madagascar day gecko green measured by the biochemical and fluorescence assays (figs. S2 to S4). (**D**) Comparison of v_{dark}, v_{light}, and k_d of bovine rhodopsin, V89F and Y172F mutants of tokay gecko UV, and S90A and F172Y mutants of Madagascar day gecko UV measured by the biochemical and fluorescence assays (figs. S2 to S4). (**E**) Comparison of the thermal activation rates (k_{th}) of bovine rhodopsin, wild type and T213V mutant of tokay gecko green, and green anole green estimated from the data in (C). (**F**) Comparison of the thermal activation rates (k_{th}) of bovine rhodopsin, wild type and V89F and Y172F mutants of tokay gecko UV, and green anole UV estimated from the data in (D). (**G**) Comparison of the thermal activation rates (k_{th}) of bovine rhodopsin, wild type and F112I mutant of Madagascar day gecko green, and tokay gecko green estimated from the data in (C). (**H**) Comparison of the thermal activation rates (k_{th}) of bovine rhodopsin, wild type and S90A and F172Y mutants of Madagascar day gecko UV, and tokay gecko UV estimated from the data in (D). All error bars represent the SEM of more than three independent measurements. * indicates a significant difference in relative rate constants between the mutants and wild type of tokay gecko green in (E) (Bonferroni, $P < 0.05/4$; ANOVA), tokay gecko UV in (F) (Bonferroni, $P < 0.05/5$; ANOVA), Madagascar day gecko green in (G) (Bonferroni, $P < 0.05/4$; ANOVA), or Madagascar day gecko UV in (H) (Bonferroni, $P < 0.05/5$; ANOVA).

gecko UV and found that S90A and F172Y mutants had significantly decreased k_d (fig. S9D). As expected, S90A and F172Y mutants of Madagascar day gecko UV had decreased thermal activation rates (by 3.6- and 2.0-fold, respectively) (Fig. 3, D and H). These results suggest that Phe[112] in Madagascar day gecko green and Ser[90] and Phe[172] in Madagascar day gecko UV mainly contribute to the re-acquisition of their high thermal activation rates approximating those of typical cone pigments. However, our mutational analysis revealed that the individual single mutations cannot perfectly explain the low thermal activation rates of nocturnal gecko cone pigments or the high thermal activation rates of diurnal gecko cone pigments. We speculate that multiple amino acid substitutions not only around the retinal but also in other regions of cone pigments can cooperatively lead to the changes of their thermal activation rates to adapt to nocturnal and diurnal activities.

Molecular mechanism for tuning of the thermal activation rates

Previous studies showed that the thermal activation rates of visual pigments were determined by two factors, the pigment's absorption maximum (λ_{max}) and the structural fluctuation of the retinal binding pocket (RBP) (open state versus closed state) (*34*, *35*). In other words, the thermal activation rates can be expressed based on the Hinshelwood distribution as follows

$$k_{th} = A \times e^{-\frac{E_a}{RT}} \sum_1^m \frac{1}{(m-1)!} \left(\frac{E_a}{RT}\right)^{m-1} \quad (2)$$

(R is the gas constant, T is absolute temperature, and m is the number of molecular vibrational modes contributing thermal energy to pigment activation), where E_a is inversely proportional to λ_{max} and pre-exponential factor A depends on the structural fluctuation of RBP. According to this framework, to assess the molecular mechanism of the regulation of k_{th}, we showed experimentally that the thermal activation rates were strongly related to k_d among all visual pigments we analyzed (*29*, *30*). This correlation can be explained by the molecular model that k_d is regulated by the structural fluctuation of RBP (*36*). In this study, we found that k_{th} and k_d of wild type and mutants of lizard and gecko cone pigments can also be plotted with a linear relationship as observed in the previous studies (Fig. 4).

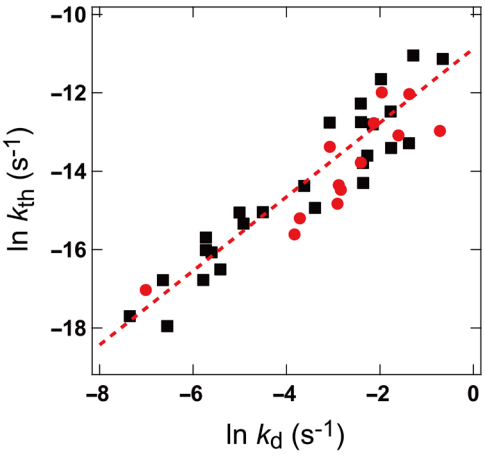

Fig. 4. Correlation between the thermal activation rates (k_{th}) and k_d of the visual pigments and their mutants. Plots of ln k_{th} and ln k_d of the visual pigments. Red circles indicate data from this study, while black squares indicate data from our previous studies (*29*, *30*). The regression line derived from all data is shown by a red dashed line. $R = 0.94$ ($P < 0.05$).

Moreover, we identified several key mutations (i.e., T213V in tokay gecko green, V89F and Y172F in tokay gecko UV, F112I in Madagascar day gecko green, and S90A and F172Y in Madagascar day gecko UV), which significantly changed both k_d and k_{th} with little spectral shift (fig. S10). This suggests that these mutations change pre-exponential factor A to regulate the thermal activation rates among lizard and gecko cone pigments. In addition to pre-exponential factor A, λ_{max}, which is inversely proportional to E_a, is also an important factor determining the thermal activation rates, as shown in Eq. 2 (*34*, *35*, *37*). λ_{max} of tokay gecko and of Madagascar day gecko greens are ~30 nm blue shifted from that of green anole green (fig. S10) (*26*). Thus, together with the decrease of A, this blue shift may also contribute to the suppression of the thermal activation rate of tokay gecko green.

In this study, we analyzed the thermal activation rates using our biochemical method (*29*–*31*). Our previous biochemical analysis showed that the thermal activation rate of mouse green-sensitive cone pigment is ~700-fold higher than that of mouse rhodopsin, and the rate of frog blue-sensitive cone pigment expressed in green rods is only ~10-fold higher than that of frog rhodopsin, which is consistent with the results obtained by the electrophysiological method (*29*, *38*, *39*). However, we note that the absolute values of the thermal activation rate estimated by our biochemical method (e.g., 2.05×10^{-8} s^{-1} for mouse rhodopsin) are ~300-fold higher than those estimated by the electrophysiological method (6.64×10^{-11} s^{-11} for mouse rhodopsin) (*29*, *34*). This inconsistency probably mainly comes from the underestimation of ν_{light} in our measurement. The catalytic rate of Gt activation by activated rhodopsin depends on not only Gt concentration but also the ratio of Gt molecules to activated rhodopsin molecules (*40*). Under the dim light condition used to achieve single-photon detection in rods, activated rhodopsin molecules are surrounded by a large excess of Gt molecules (~3000 Gt/Rh*), which allows the rhodopsin molecules to activate Gt with the maximal catalytic rate (ν_{light} = ~600 s^{-1}) (*40*, *41*). This ν_{light} value is equivalent to the reported finding that a photoactivated rhodopsin can activate 12 to 14 Gt molecules in the single-photon response of mouse rods, where the photoactivated rhodopsin is rapidly inactivated in less than 0.08 s (*42*). In our assay condition of ν_{dark}, Gt concentration (Gt: 1 μM) is comparable to that in rods (Gt: ~0.7 μM) (*40*), and the population of thermally activated rhodopsin is estimated to be ~8.5 pM and the Gt/R* ratio is ~120,000, where thermally activated rhodopsin can activate Gt with the maximal catalytic rate, such as in intact rods. By contrast, we optimized the assay condition to accurately measure ν_{light} using a larger amount of detergent-purified visual pigments (20 nM), where the Gt/Rh* ratio (1 μM/20 nM = 50) is much lower than that in the assay condition of ν_{dark}. In this condition, ν_{light} of rhodopsin is estimated to be 2.39 s^{-1}, which implies a low catalytic rate in the background, where Rh* rapidly depletes Gt due to the low Gt/R* ratio. Note that rhodopsin embedded in a nanoscale lipid bilayer (nanodisc) shows a similar ν_{light} value (7.03 s^{-1}) in the similar low Gt/Rh* ratio (*43*). Thus, according to the previous study (*40*), we presume that the low Gt/Rh* ratio results in the low catalytic rate in the assay condition of ν_{light} to cause the underestimation of ν_{light}. In addition, our measurement of k_d revealed that k_d of visual pigments in the detergent micelles was ~2-fold larger than that in the nanoscale lipid bilayer (*43*, *44*). Together, the combination of ~250-fold underestimation of ν_{light} value and ~2-fold overestimation of k_d value in our measurement leads to higher k_{th} in Eq. 1, which can explain the difference in the thermal activation rate estimated using the electrophysiological and biochemical methods. However, there is an exceptional case in which effects of E122Q mutation on the thermal activation rate of bovine rhodopsin measured by the biochemical method are inconsistent with those of mouse rhodopsin measured by the electrophysiological method (*29*, *37*). Thus, the electrophysiological measurement of the dark noise of intact photoreceptor cells in the gecko retinas is necessary to confirm the thermal activation rates of gecko cone pigments, which will be our future work.

The implication of evolutionary changes of the thermal activation rates in gecko cone pigments

In the nocturnal gecko retina, individual types of cone pigments are predominantly expressed in different types of rods that show the different spectral sensitivities (*45*). Previous behavioral analyses showed that nocturnal geckos can distinguish colors under scotopic conditions (*46*, *47*), which can be explained by the low noise level of nocturnal gecko rods similar to that of normal rods containing rhodopsin. Our analysis indicated that nocturnal tokay gecko cone pigments decreased their thermal activation rates to mimic that of rhodopsin during the transmutation process of the morphology of the photoreceptor cells, which suppresses the discrete noise level of rods in the nocturnal gecko. The sensitivity of scotopic vision in nocturnal geckos probably also benefits from a thermally stable PDE6, which keeps the continuous noise low. In general, rod PDE6 protein consists of a catalytic heterodimer of PDE6a and PDE6b subunits with two identical inhibitory subunits, whereas cone PDE6 protein contains a catalytic homodimer of two PDE6c subunits (*21*). However, nocturnal geckos lost the *PDE6A* and *PDE6B* genes, and thus, it is expected that nocturnal geckos express PDE6c proteins in their rods (*21*, *27*, *48*). Moreover, the catalytic activity of the nocturnal gecko PDE6c protein is comparable to that of mammalian rod PDE6a/b protein (*20*), which suggests that the molecular properties of the nocturnal gecko PDE6c protein changed to mimic that of the PDE6a/b protein. Therefore, we speculate that nocturnal geckos have suppressed the spontaneous activation rates of PDE6c, similar to typical rod

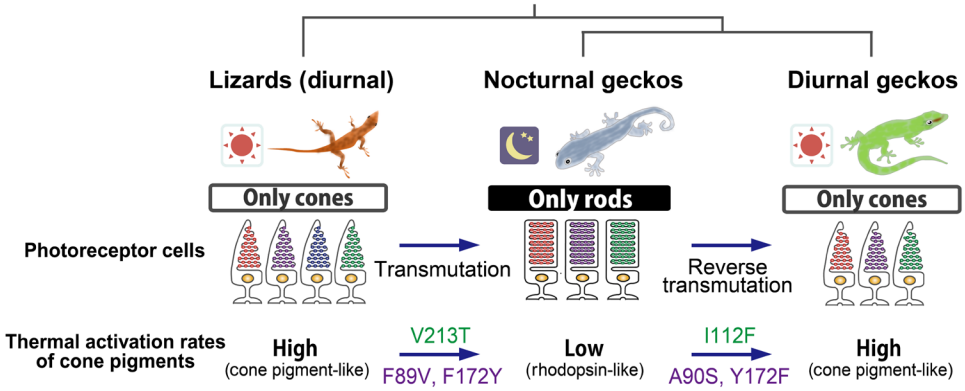

Fig. 5. Evolutionary relationship of photoreceptor cells and visual pigments in lizards and geckos. It is hypothesized that the common ancestor of geckos was diversified from diurnal lizards to acquire nocturnality with the transmutation from cones into rods, and subsequently, diurnal geckos have evolved from nocturnal species with the retransmutation from rods into cones (*27*, *49*).

PDE6a/b, to achieve the low continuous noise level in their transmuted rods. Summarizing the above, the acquisition of the low thermal activation rates of nocturnal gecko cone pigments could provide the molecular basis of the low noise level of their transmuted rods for scotopic color vision (Fig. 5). Our previous study indicated that frog blue-sensitive cone pigments expressed in green rods exhibit low thermal activation rates as a result of a single amino acid replacement at position 47, which underlies scotopic color vision with normal red rods containing green-sensitive rhodopsin (*30*). We propose that scotopic color vision of frogs and geckos is attributable to the convergent evolution of cone pigments expressed uniquely in rods by the suppression of their thermal activation rates.

Since geckos consist mostly of nocturnal species and diurnal species are independently derived from distinct clades, it is proposed that nocturnality was acquired early in the gecko evolutionary history, and diurnal species (e.g., Madagascar day gecko) have evolved from nocturnal ancestors (*27*, *49*). In the diurnal gecko retina, individual types of cones predominantly express the different types of cone pigments that show different spectral sensitivities, which allow them to distinguish colors under photopic conditions (*50*). This adaptation to photopic conditions can be explained by the high noise level of diurnal gecko cones, similar to that of normal cones. Thus, diurnal gecko cones needed to increase the pigment-related noise level and/or continuous noise level during the transmutation process from ancestral rods that exhibited low levels of both discrete and continuous noises. Our analysis indicated that diurnal Madagascar day gecko cone pigments have increased their thermal activation rates during the evolutionary process from an ancestral nocturnal gecko. The high thermal activation rates of cone pigments achieve the high pigment-related noise level of cones in the diurnal gecko. We speculate that the increase of the pigment-related noise level in cones contributed to the photopic vision of diurnal geckos without the increase of the continuous noise level according to the retransmutation from rods to cones (Fig. 5). By contrast, the diurnal western ribbon snake has not increased the thermal activation rates of rhodopsin expressed in cones (fig. S5), which leads to low level of the pigment-related noise in cones. Since the high noise level of cones sets the limit on the sensitivity of photopic vision, it is expected that diurnal western ribbon snake cones that express rhodopsin exhibit an increased level of the continuous noise by high spontaneous activation rates of PDE6 proteins. Therefore, diurnal geckos and snakes have possibly adopted different strategies to acquire the high noise level of their transmuted cones for the photopic environment. It is also possible that the high thermal activation rates of diurnal gecko cone pigments result from relaxed natural selection for thermal activation rates of cone pigments. Moreover, the increase of thermal activation rates of diurnal gecko cone pigments corresponds to the rapid release of all-trans retinal from photoactivated pigments (high k_d) (Fig. 4), which leads to the fast recovery of the dark current of cones for photopic vision. In this context, the high thermal activation rates of diurnal gecko cone pigments might result in the fast cycling of the pigments.

During the stepwise transmutation process of the morphology of the photoreceptor cells, nocturnal geckos uniquely acquired low thermal activation rates of cone pigments expressed in rods in the genetic background that does not contain the rhodopsin gene, and subsequently, diurnal geckos recovered the high thermal activation rates of cone pigments to use them in cones. Geckos would thus have evolutionarily tuned their visual pigments through several amino acid mutations to adapt to the changes of their activity rhythm. In addition to our molecular characterization of visual pigments, physiological characterization of the dark noise and the detection threshold in nocturnal and diurnal gecko species will lead to further understanding of the adaptation process for the photic environment in geckos.

MATERIALS AND METHODS

Heterologous expression and purification of the visual pigments

The cDNA of bovine rhodopsin (K00506) was inserted into the mammalian expression vector pUSRα. The cDNAs of other visual pigments—green anole green (AF134191), tokay gecko green (M92035), Madagascar day gecko green (AAD25918), green anole UV (AF134194), tokay gecko UV (AAG61163), Madagascar day gecko UV (AAD45183), tiger salamander UV (AF038948), western ribbon snake rhodopsin (KU306726), and western ribbon snake UV (KU306728)—were tagged by the epitope sequence of the anti–bovine rhodopsin monoclonal antibody Rho1D4 at the C terminus and inserted into the mammalian expression vector pMT4 (*51*).

Expression of the visual pigments in human embryonic kidney (HEK) 293 cells and sample preparation of the visual pigments were performed as previously described (*29*). The cell membranes expressing the visual pigments were divided into two aliquots. One was regenerated by 11-cis-retinal and 7-membered-ring 11-cis-retinal (7mr) (*29*, *52*), and the other was regenerated by only 7mr. After regeneration, they were solubilized by Buffer A [50 mM Hepes and 140 mM NaCl (pH 6.5)] containing 1% dodecyl maltoside (DDM) and purified using Rho1D4-conjugated agarose. The purified visual pigments were eluted with 0.02% DDM in Buffer A containing the synthetic C-terminal peptide of bovine rhodopsin. All of the experiments after reconstitution of the visual pigments with 11-cis-retinal were performed in complete darkness using an infrared night vision device. We refer to the purified samples regenerated by both 11-cis-retinal and 7mr or only 7mr as "pigment name-n" or "pigment name-7mr," respectively. We confirmed that the concentrations of the visual pigments contained in the two samples were similar by Western blotting analysis as previously described (*29*, *30*). The samples of the visual pigments for the spectroscopic measurement were regenerated with 11-cis-retinal and purified as described above.

Measurement of v_{dark}, v_{light}, and k_d and estimation of k_{th}

v_{dark} was measured by the [^{35}S]GTPγS binding assay in complete darkness using an infrared night vision device as previously described (*29*, *30*). The assay mixture consisted of 300 nM pigments (1875 nM for green anole UV, tokay gecko UV, Madagascar day gecko UV, tiger salamander UV, and western ribbon snake UV to increase signal-to-signal ratio), 1 μM Gt, 5 μM GTPγS, 25 nM [^{35}S]GTPγS, 0.015% DDM, 50 mM Hepes (pH 6.5), 140 mM NaCl, 5.8 mM $MgCl_2$, and 1 mM dithiothreitol (DTT). Experimental data were fitted by a single exponential function, and v_{dark} was estimated by the difference between the initial rates between two samples (pigment name-n and pigment name-7mr). v_{light} was measured by a fluorescence assay as previously described (*43*, *53*). The assay mixture consisted of 20 nM pigments (125 nM for green anole UV, tokay gecko UV, Madagascar day gecko UV, tiger salamander UV, and western ribbon snake UV to increase the signal-to-noise ratio), 0 or 1 μM Gt, 5 μM GTPγS, 0.015% DDM, 50 mM Hepes (pH 6.5), 140 mM NaCl, 5.8 mM $MgCl_2$, and 1 mM DTT. Experimental data were fitted by a single exponential function, and v_{light} was estimated as previously described (*43*, *44*). k_d was measured by a fluorescence assay as previously described (*44*, *54*). The assay mixture consisted of 20 nM pigments (60 nM for green anole UV, tokay gecko UV, Madagascar day gecko UV, tiger salamander UV, and western ribbon snake UV to increase the signal-to-noise ratio), 5 μM GTPγS, 0.015% DDM, 50 mM Hepes (pH 6.5), 140 mM NaCl, 5.8 mM $MgCl_2$, and 1 mM DTT. Experimental data were fitted by a single exponential function to estimate k_d. According to our previous reports, the thermal activation rates (k_{th}) were calculated using Eq. 1 by using three experimentally determined values (v_{dark}, v_{light}, and k_d).

Western blotting

Extracts from visual pigment–transfected HEK293 cells were subjected to SDS–polyacrylamide gel electrophoresis, transferred onto a polyvinylidene difluoride membrane, and probed with Rho1D4. Immunoreactive proteins were detected using ECL (GE Healthcare) and visualized using a luminescent image analyzer (LAS 4000 mini, GE Healthcare) as previously described (*30*).

Spectroscopic measurements

Absorption spectra of the samples were recorded with a UV-visible spectrophotometer (Shimadzu UV-2450, UV-2400). Samples were kept at 0°C using a cell holder equipped with a temperature-controlled circulating water bath.

SUPPLEMENTARY MATERIALS

Supplementary material for this article is available at https://science.org/doi/10.1126/sciadv.abj1316

View/request a protocol for this paper from *Bio-protocol*.

REFERENCES AND NOTES

1. Y. Fu, K. W. Yau, Phototransduction in mouse rods and cones. *Pflugers Arch.* **454**, 805–819 (2007).
2. S. Kawamura, S. Tachibanaki, Rod and cone photoreceptors: Molecular basis of the difference in their physiology. *Comp. Biochem. Physiol. A Mol. Integr. Physiol.* **150**, 369–377 (2008).
3. S. Hecht, S. Shlaer, M. H. Pirenne, Energy, quanta, and vision. *J. Gen. Physiol.* **25**, 819–840 (1942).
4. G. D. Field, A. P. Sampath, F. Rieke, Retinal processing near absolute threshold: From behavior to mechanism. *Annu. Rev. Physiol.* **67**, 491–514 (2005).
5. J. Pahlberg, A. P. Sampath, Visual threshold is set by linear and nonlinear mechanisms in the retina that mitigate noise: How neural circuits in the retina improve the signal-to-noise ratio of the single-photon response. *Bioessays* **33**, 438–447 (2011).
6. D. A. Baylor, G. Matthews, K. W. Yau, Two components of electrical dark noise in toad retinal rod outer segments. *J. Physiol.* **309**, 591–621 (1980).
7. P. Ala-Laurila, K. Donner, R. K. Crouch, M. C. Cornwall, Chromophore switch from 11-*cis*-dehydroretinal (A2) to 11-*cis*-retinal (A1) decreases dark noise in salamander red rods. *J. Physiol.* **585**, 57–74 (2007).
8. F. Rieke, D. A. Baylor, Molecular origin of continuous dark noise in rod photoreceptors. *Biophys. J.* **71**, 2553–2572 (1996).
9. J. M. Angueyra, F. Rieke, Origin and effect of phototransduction noise in primate cone photoreceptors. *Nat. Neurosci.* **16**, 1692–1700 (2013).
10. A. C. Aho, K. Donner, C. Hyden, L. O. Larsen, T. Reuter, Low retinal noise in animals with low body temperature allows high visual sensitivity. *Nature* **334**, 348–350 (1988).
11. G. D. Field, F. Rieke, Nonlinear signal transfer from mouse rods to bipolar cells and implications for visual sensitivity. *Neuron* **34**, 773–785 (2002).
12. F. Naarendorp, T. M. Esdaille, S. M. Banden, J. Andrews-Labenski, O. P. Gross, E. N. Pugh Jr., Dark light, rod saturation, and the absolute and incremental sensitivity of mouse cone vision. *J. Neurosci.* **30**, 12495–12507 (2010).
13. A. Kelber, C. Yovanovich, P. Olsson, Thresholds and noise limitations of colour vision in dim light. *Philos. Trans. R. Soc. Lond. B Biol. Sci.* **372**, 20160065 (2017).
14. F. Rieke, D. A. Baylor, Origin and functional impact of dark noise in retinal cones. *Neuron* **26**, 181–186 (2000).
15. V. Kefalov, Y. Fu, N. Marsh-Armstrong, K. W. Yau, Role of visual pigment properties in rod and cone phototransduction. *Nature* **425**, 526–531 (2003).
16. G. L. Walls, The reptilian retina: I. A new concept of visual-cell evolution. *Am. J. Ophthalmol.* **17**, 892–915 (1934).
17. C. Pedler, R. Tilly, The nature of the Gecko visual cell: A light and electron microscopic study. *Vision Res.* **4**, 499–510 (1964).
18. K. Tansley, The gecko retina. *Vision Res.* **4**, 33–37 (1964).
19. D. Kojima, T. Okano, Y. Fukada, Y. Shichida, T. Yoshizawa, T. G. Ebrey, Cone visual pigments are present in gecko rod cells. *Proc. Natl. Acad. Sci. U.S.A.* **89**, 6841–6845 (1992).
20. X. Zhang, T. G. Wensel, C. Yuan, Tokay gecko photoreceptors achieve rod-like physiology with cone-like proteins. *Photochem. Photobiol.* **82**, 1452–1460 (2006).
21. D. Lagman, I. E. Franzen, J. Eggert, D. Larhammar, X. M. Abalo, Evolution and expression of the phosphodiesterase 6 genes unveils vertebrate novelty to control photosensitivity. *BMC Evol. Biol.* **16**, 124 (2016).
22. S. Kawamura, S. Yokoyama, Expression of visual and nonvisual opsins in American chameleon. *Vision Res.* **37**, 1867–1871 (1997).
23. E. R. Loew, L. J. Fleishman, R. G. Foster, I. Provencio, Visual pigments and oil droplets in diurnal lizards: A comparative study of Caribbean anoles. *J. Exp. Biol.* **205**, 927–938 (2002).
24. Y. Liu, Q. Zhou, Y. Wang, L. Luo, J. Yang, L. Yang, M. Liu, Y. Li, T. Qian, Y. Zheng, M. Li, J. Li, Y. Gu, Z. Han, M. Xu, Y. Wang, C. Zhu, B. Yu, Y. Yang, F. Ding, J. Jiang, H. Yang, X. Gu, *Gekko japonicus* genome reveals evolution of adhesive toe pads and tail regeneration. *Nat. Commun.* **6**, 10033 (2015).

25. Y. Hara, M. Takeuchi, Y. Kageyama, K. Tatsumi, M. Hibi, H. Kiyonari, S. Kuraku, Madagascar ground gecko genome analysis characterizes asymmetric fates of duplicated genes. *BMC Biol.* **16**, 40 (2018).
26. S. Yokoyama, N. S. Blow, Molecular evolution of the cone visual pigments in the pure rod-retina of the nocturnal gecko, *Gekko gekko*. *Gene* **276**, 117–125 (2001).
27. B. J. Pinto, S. V. Nielsen, T. Gamble, Transcriptomic data support a nocturnal bottleneck in the ancestor of gecko lizards. *Mol. Phylogenet. Evol.* **141**, 106639 (2019).
28. Y. Taniguchi, O. Hisatomi, M. Yoshida, F. Tokunaga, Evolution of visual pigments in geckos. *FEBS Lett.* **445**, 36–40 (1999).
29. M. Yanagawa, K. Kojima, T. Yamashita, Y. Imamoto, T. Matsuyama, K. Nakanishi, Y. Yamano, A. Wada, Y. Sako, Y. Shichida, Origin of the low thermal isomerization rate of rhodopsin chromophore. *Sci. Rep.* **5**, 11081 (2015).
30. K. Kojima, Y. Matsutani, T. Yamashita, M. Yanagawa, Y. Imamoto, Y. Yamano, A. Wada, O. Hisatomi, K. Nishikawa, K. Sakurai, Y. Shichida, Adaptation of cone pigments found in green rods for scotopic vision through a single amino acid mutation. *Proc. Natl. Acad. Sci. U.S.A.* **114**, 5437–5442 (2017).
31. K. Sato, T. Yamashita, K. Kojima, K. Sakai, Y. Matsutani, M. Yanagawa, Y. Yamano, A. Wada, N. Iwabe, H. Ohuchi, Y. Shichida, Pinopsin evolved as the ancestral dim-light visual opsin in vertebrates. *Commun. Biol.* **1**, 156 (2018).
32. B. F. Simões, F. L. Sampaio, E. R. Loew, K. L. Sanders, R. N. Fisher, N. S. Hart, D. M. Hunt, J. C. Partridge, D. J. Gower, Multiple rod–cone and cone–rod photoreceptor transmutations in snakes: Evidence from visual opsin gene expression. *Proc. Biol. Sci. B* **283**, 20152624 (2016).
33. R. K. Schott, J. Müller, C. G. Yang, N. Bhattacharyya, N. Chan, M. Xu, J. M. Morrow, A.-H. Ghenu, E. R. Loew, V. Tropepe, B. S. Chang, Evolutionary transformation of rod photoreceptors in the all-cone retina of a diurnal garter snake. *Proc. Natl. Acad. Sci. U.S.A.* **113**, 356–361 (2016).
34. D.-G. Luo, W. W. Yue, P. Ala-Laurila, K.-W. Yau, Activation of visual pigments by light and heat. *Science* **332**, 1307–1312 (2011).
35. P. Ala-Laurila, K. Donner, A. Koskelainen, Thermal activation and photoactivation of visual pigments. *Biophys. J.* **86**, 3653–3662 (2004).
36. R. Piechnick, E. Ritter, P. W. Hildebrand, O. P. Ernst, P. Scheerer, K. P. Hofmann, M. Heck, Effect of channel mutations on the uptake and release of the retinal ligand in opsin. *Proc. Natl. Acad. Sci. U.S.A.* **109**, 5247–5252 (2012).
37. W. W. Yue, R. Frederiksen, X. Ren, D.-G. Luo, T. Yamashita, Y. Shichida, M. C. Cornwall, K.-W. Yau, Spontaneous activation of visual pigments in relation to openness/closedness of chromophore-binding pocket. *eLife* **6**, e18492 (2017).
38. K. Sakurai, A. Onishi, H. Imai, O. Chisaka, Y. Ueda, J. Usukura, K. Nakatani, Y. Shichida, Physiological properties of rod photoreceptor cells in green-sensitive cone pigment knock-in mice. *J. Gen. Physiol.* **130**, 21–40 (2007).
39. G. Matthews, Dark noise in the outer segment membrane current of green rod photoreceptors from toad retina. *J. Physiol.* **349**, 607–618 (1984).
40. M. Heck, K. P. Hofmann, Maximal rate and nucleotide dependence of rhodopsin-catalyzed transducin activation: Initial rate analysis based on a double displacement mechanism. *J. Biol. Chem.* **276**, 10000–10009 (2001).
41. T. M. Vuong, M. Chabre, L. Stryer, Millisecond activation of transducin in the cyclic nucleotide cascade of vision. *Nature* **311**, 659–661 (1984).
42. W. W. S. Yue, D. Silverman, X. Ren, R. Frederiksen, K. Sakai, T. Yamashita, Y. Shichida, M. C. Cornwall, J. Chen, K. W. Yau, Elementary response triggered by transducin in retinal rods. *Proc. Natl. Acad. Sci. U.S.A.* **116**, 5144–5153 (2019).
43. K. Kojima, Y. Imamoto, R. Maeda, T. Yamashita, Y. Shichida, Rod visual pigment optimizes active state to achieve efficient G protein activation as compared with cone visual pigments. *J. Biol. Chem.* **289**, 5061–5073 (2014).
44. Y. Imamoto, I. Seki, T. Yamashita, Y. Shichida, Efficiencies of activation of transducin by cone and rod visual pigments. *Biochemistry* **52**, 3010–3018 (2013).
45. F. Crescitelli, H. J. Dartnall, E. R. Loew, The gecko visual pigments: A microspectrophotometric study. *J. Physiol.* **268**, 559–573 (1977).
46. L. S. Roth, A. Kelber, Nocturnal colour vision in geckos. *Proc. Biol. Sci.* **271**, S485–S487 (2004).
47. A. Kelber, L. S. Roth, Nocturnal colour vision—Not as rare as we might think. *J. Exp. Biol.* **209**, 781–788 (2006).
48. R. K. Schott, N. Bhattacharyya, B. S. W. Chang, Evolutionary signatures of photoreceptor transmutation in geckos reveal potential adaptation and convergence with snakes. *Evolution* **73**, 1958–1971 (2019).
49. T. Gamble, E. Greenbaum, T. R. Jackman, A. M. Bauer, Into the light: Diurnality has evolved multiple times in geckos. *Biol. J. Linn. Soc.* **115**, 896–910 (2015).
50. J. M. Ellingson, L. J. Fleishman, E. R. Loew, Visual pigments and spectral sensitivity of the diurnal gecko *Gonatodes albogularis*. *J. Comp. Physiol. A* **177**, 559–567 (1995).
51. D. D. Oprian, R. S. Molday, R. J. Kaufman, H. G. Khorana, Expression of a synthetic bovine rhodopsin gene in monkey kidney cells. *Proc. Natl. Acad. Sci. U.S.A.* **84**, 8874–8878 (1987).
52. H. Akita, S. P. Tanis, M. Adams, V. Balogh-Nair, K. Nakanishi, Nonbleachable rhodopsins retaining the full natural chromophore. *J. Am. Chem. Soc.* **102**, 6370–6372 (1980).
53. K. Kojima, T. Yamashita, Y. Imamoto, T. G. Kusakabe, M. Tsuda, Y. Shichida, Evolutionary steps involving counterion displacement in a tunicate opsin. *Proc. Natl. Acad. Sci. U.S.A.* **114**, 6028–6033 (2017).
54. T. Matsuyama, T. Yamashita, H. Imai, Y. Shichida, Covalent bond between ligand and receptor required for efficient activation in rhodopsin. *J. Biol. Chem.* **285**, 8114–8121 (2010).

Acknowledgments: We thank E. Nakajima for critical reading of the manuscript. We also thank R. S. Molday for the gift of a Rho1D4-producing hybridoma and O. Hisatomi for providing cDNAs of Madagascar day gecko green– and UV–sensitive cone pigments. **Funding:** This work was supported in part by Grants-in-Aid for Scientific Research of MEXT to K.K. (15J02054), Y.I. (19K21848), Y.S. (16H02515), and T.Y. (16K07437); CREST, JST JPMJCR1753 (to T.Y.); a grant from the Kyoto University Foundation (T.Y.); and a grant from the Takeda Science Foundation (to T.Y.). **Author contributions:** K.K., Y.S., and T.Y. designed the research. K.K. and Y.M. performed the research. M.Y., Y.I., Y.Y., and A.W. contributed new reagents and analytic tools. K.K., Y.S., and T.Y. analyzed data. K.K., Y.S., and T.Y. wrote the manuscript with editing performed by all authors. **Competing interests:** The authors declare that they have no competing interests. **Data and materials availability:** All data needed to evaluate the conclusions in the paper are present in the paper and/or the Supplementary Materials.

Submitted 23 April 2021
Accepted 11 August 2021
Published 1 October 2021
10.1126/sciadv.abj1316

Citation: K. Kojima, Y. Matsutani, M. Yanagawa, Y. Imamoto, Y. Yamano, A. Wada, Y. Shichida, T. Yamashita, Evolutionary adaptation of visual pigments in geckos for their photic environment. *Sci. Adv.* **7**, eabj1316 (2021).

Evolutionary adaptation of visual pigments in geckos for their photic environment

Keiichi KojimaYuki MatsutaniMasataka YanagawaYasushi ImamotoYumiko YamanoAkimori WadaYoshinori ShichidaTakahiro Yamashita

Sci. Adv., 7 (40), eabj1316. • DOI: 10.1126/sciadv.abj1316